

Quantum Assisted Simulator

Kishor Bharti^{1,*} and Tobias Haug^{1,†}

¹*Centre for Quantum Technologies, National University of Singapore 117543, Singapore*

Quantum simulation offers a possibility to explore the exponentially large configuration space of quantum mechanical systems and thus help us study poorly understood topics such as high-temperature superconductivity and drug design. Here, we provide a novel hybrid quantum-classical algorithm for simulating the dynamics of quantum systems. Without loss of generality, the Hamiltonian is assumed to be a linear combination of unitaries and the Ansatz wavefunction is taken as a linear combination of quantum states. The quantum states are fixed, and the combination parameters are variationally adjusted. Unlike existing variational quantum simulation algorithms, our algorithm does not require any classical-quantum feedback loop and by construction bypasses the barren plateau problem. Moreover, our algorithm does not require any complicated measurements, such as the Hadamard test. The entire framework is compatible with existing experimental capabilities and thus can be implemented immediately. We also provide an extension of our algorithm to imaginary time evolution.

The near-term success of the second quantum revolution critically depends on the practical applications of noisy intermediate-scale quantum (NISQ) [1, 2] devices. Though experimental demonstration of “quantum supremacy” has induced widespread hope [3], the essential question regarding how to translate such breakthroughs into quantum advantages for practical use-cases remains unsolved. The search for the “killer app” for NISQ devices continues, with potential areas of application being solid-state physics, quantum chemistry and combinatorial optimization. Most of the problems from the aforementioned areas can be mapped to Hamiltonian ground state problem and the simulation of quantum dynamics. Variational classical simulation (VCS) techniques have been suggested to handle static problems in estimating the ground state and ground state energy of a Hamiltonian, as well as dynamical problems in simulating the time evolution (real as well as imaginary) of quantum systems. However, for problems involving exponentially large Hilbert spaces, VCS in general fails to provide the desired solution.

The canonical NISQ era algorithm for approximating the ground state and ground state energy of a Hamiltonian is variational quantum eigensolver (VQE) [4–11]. The aforementioned algorithm is hybrid (quantum-classical) in nature and employs a classical optimizer to tune the parameters of a parametric quantum circuit. The loss function or the gradient of the loss function is evaluated via a quantum device. The classical optimization landscape corresponding to VQE can be highly non-convex and is in general uncharacterized, rendering any proper theoretical study difficult. Moreover, the recent results on the appearance of the barren plateau as the hardware noise, amount of entanglement or number of qubits increase, has led to genuine concerns regarding the fate of VQE [12–17]. To tackle the existing challenges in VQE, quantum assisted eigensolver (QAE) [18]

and iterative quantum assisted eigensolver (IQAE) [19] have been recently proposed in the literature. The classical optimization program corresponding to these algorithms is a quadratically constrained quadratic program with single equality constraint, which is a well characterized optimization program. In particular, the IQAE algorithm provides a systematic path to build Ansatz, bypasses the barren plateau problem and can be efficiently implemented on existing hardware.

The broader task of simulating quantum dynamics is challenging as the Hilbert space dimension increases exponentially, which poses a considerable bottleneck to the study and design of new drugs, catalysts, and materials. A universal quantum computer, with millions of qubits with noise levels beneath a critical threshold offers a possibility to simulate the dynamics. Simulation algorithms such as Trotterization usually require many quantum gates, which most likely would require the use of fault tolerant quantum computers to implement [20]. However, most likely fault-tolerant quantum computers will not be available in the near future. Thus, to harness the potential of NISQ hardware, variational quantum simulation (VQS) algorithms have been suggested in literature [21–23]. The algorithm is hybrid quantum-classical in nature and utilizes dynamical variational principles to update the parameters of a parametric quantum circuit, such that the Ansatz evolution emulates quantum evolution. The VQS algorithm, however, shares issues faced by VQE such as the barren plateau problem. Moreover, it requires complicated measurements involving controlled unitaries, which may not be viable in the NISQ era. Furthermore, the Ansatz is not chosen in a systematic way in VQS and typically requires adjustable parameters to be real-valued [23].

In this work, we provide a novel hybrid quantum-classical algorithm for simulating the dynamics of quantum systems. We refer to our algorithm as quantum assisted simulator (QAS) algorithm. The Hamiltonian is assumed to be a linear combination of unitaries, and the Ansatz is a linear combination of quantum states. The combination coefficients are complex-valued, in gen-

* kishor.bharti@gmail.com

† tobiasxhaug@gmail.com

eral. Unlike existing variational quantum simulation algorithms, our algorithm does not mandate any classical-quantum feedback loop. By construction, the algorithm circumvents the barren plateau problem. Our algorithm does not demand any complicated measurement involving controlled unitaries. The entire framework is compatible with existing experimental capabilities and thus can be implemented immediately. We also discuss the extension of our algorithm to imaginary time evolution.

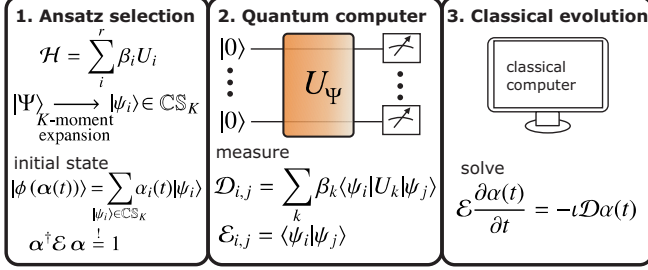


FIG. 1. The Quantum Assisted Simulator (QAS) algorithm consists of three steps. The first step involves the selection of the Ansatz. The Ansatz is represented as a linear combination of cumulative K -moment states (see Definition 1), for some choice of non-negative integer K . The second step involves the computation of overlap matrices on a quantum computer, which can be performed efficiently, without the requirement of any complicated measurement, using the techniques in Appendix E. After the overlap matrices have been computed, the differential equation corresponding to equation (15) is solved on a classical computer. Unlike existing variational quantum simulation algorithms, QAS does not mandate any classical-quantum feedback loop.

QAS Algorithm—The time evolution of a closed system, represented by the time-dependent quantum state $|\psi(t)\rangle$ for Hamiltonian H is given by

$$\frac{d|\psi(t)\rangle}{dt} = -\iota H |\psi(t)\rangle. \quad (1)$$

Let us consider the Hamiltonian H as a linear combination of r unitaries

$$H = \sum_{i=1}^r \beta_i U_i, \quad (2)$$

where the combination coefficients $\beta_i \in \mathbb{C}$ and the N -qubit unitaries $U_i \in \text{SU}(2^N \equiv \mathcal{N})$, for $i \in \{1, 2, \dots, r\}$. Moreover, each unitary acts non-trivially on at most $\mathcal{O}(\text{poly}(\log N))$ qubits. If the unitaries in equation (2) are tensored Pauli matrices, we do not need the aforementioned $\mathcal{O}(\text{poly}(\log N))$ constraint. Let us consider the Ansatz state as time dependent linear combination of m quantum states $\{|\psi_i\rangle\}_i$

$$|\phi(\alpha(t))\rangle = \sum_{i=0}^{m-1} \alpha_i(t) |\psi_i\rangle, \quad (3)$$

for $\alpha_i(t) \in \mathbb{C}$. Normalization of the Ansatz wavefunction $\langle \phi(\alpha) | \phi(\alpha) \rangle = 1$ is achieved by demanding

$$\alpha^\dagger \mathcal{E} \alpha = 1, \quad (4)$$

where

$$\mathcal{E}_{i,j} = \langle \psi_i | \psi_j \rangle. \quad (5)$$

Using Dirac and Frenkel variational principle [24, 25], we get

$$\langle \delta \phi(\alpha(t)) | \left(\frac{d}{dt} + \iota H \right) | \phi(\alpha) \rangle = 0, \quad (6)$$

where

$$\langle \delta \phi(\alpha(t)) | = \sum_i \frac{\partial \langle \phi(\alpha(t)) |}{\partial \alpha_i} \delta \alpha_i(t) \quad (7)$$

The evolution of $\alpha(t)$ can be solved to be

$$\sum_j \mathcal{E}_{i,j} \dot{\alpha}_j = -\iota \mathcal{C}_i, \quad (8)$$

where \mathcal{E} and \mathcal{C} are

$$\mathcal{E}_{i,j} = \frac{\partial \langle \phi(\alpha(t)) |}{\partial \alpha_i} \frac{\partial | \phi(\alpha(t)) \rangle}{\partial \alpha_j}, \quad (9)$$

$$\mathcal{C}_i = \sum_j \alpha_j(t) \frac{\partial \langle \phi(\alpha(t)) |}{\partial \alpha_i} H | \psi_j \rangle. \quad (10)$$

Using equation 2, we define

$$\mathcal{D}_{i,j} = \sum_k \beta_k \langle \psi_i | U_k | \psi_j \rangle. \quad (11)$$

Notice that

$$\frac{\partial | \phi(\alpha) \rangle}{\partial \alpha_j} = \frac{\partial \sum_{i=0}^{m-1} \alpha_i(t) | \psi_i \rangle}{\partial \alpha_j} \quad (12)$$

$$\implies \frac{\partial | \phi(\alpha) \rangle}{\partial \alpha_j} = | \psi_j \rangle. \quad (13)$$

Thus, we identify \mathcal{E} of Eq.(9) and Eq.(5) as being identical and

$$\mathcal{C}_i = \sum_j \mathcal{D}_{i,j} \alpha_j(t). \quad (14)$$

Finally, we have

$$\mathcal{E} \frac{\partial \alpha(t)}{\partial t} = -\iota \mathcal{D} \alpha(t). \quad (15)$$

Thus, one can solve for $\dot{\alpha}_j(t)$ and hence update the parameters as

$$\alpha_j(t + \delta t) = \alpha_j(t) + \dot{\alpha}_j \delta t, \quad (16)$$

for an evolution corresponding to time δt . It is easy to show that the evolution keeps $\alpha(t)$ normalized according to Eq.(4). Similarly, we can define the QAS algorithm for imaginary time evolution by substituting t with $-i\tau$ in Eq.(1). See Appendix C for details.

For pedagogical reasons, we use the notion of K -moment states and cumulative K -moment states [19].

Definition 1. Given a set of unitaries $\mathbb{U} \equiv \{U_i\}_{i=1}^r$, a positive integer K and some quantum state $|\psi\rangle$, K -moment states is the set of quantum states of the form $\{U_{i_K} \cdots U_{i_2} U_{i_1} |\psi\rangle\}_i$ for $U_{i_l} \in \mathbb{U}$. We denote the aforementioned set by \mathbb{S}_K . The singleton set $\{|\psi\rangle\}$ will be referred to as the 0-moment state (denoted by \mathbb{S}_0 .) The cumulative K -moment states \mathbb{CS}_K is defined to be $\mathbb{CS}_K \equiv \cup_{j=0}^K \mathbb{S}_j$.

For example, the set of 1-moment states is given by $\{U_i |\psi\rangle\}_{i=1}^r$, for a given initial state $|\psi\rangle$ and the unitaries $\{U_i\}_{i=1}^r$ which define the Hamiltonian H . The set of cumulative 1-moment states is given by $\mathbb{CS}_1 = \{|\psi\rangle\} \cup \{U_i |\psi\rangle\}_{i=1}^r$, and the set describing cumulative K -moment states is $\mathbb{CS}_K = \{|\psi\rangle\} \cup \{U_{i_1} |\psi\rangle\}_{i_1=1}^r \cup \cdots \cup \{U_{i_K} \cdots U_{i_1} |\psi\rangle\}_{i_1=1, \dots, i_K=1}^r$.

The QAS algorithm involves three steps (see Fig.1 for pictorial synopsis).

1. Ansatz selection
2. Calculation of the overlap matrices (\mathcal{D} and \mathcal{E}) on a quantum computer
3. Solving the differential equation and parameter update using equations 15 and 16 on a classical computer

The first step of the QAS algorithm is crucial and heavily determines the accuracy of the algorithm. We consider our Ansatz to be a linear combination of cumulative K -moment states, i.e.,

$$|\phi(\alpha(t))\rangle = \sum_{|\psi_i\rangle \in \mathbb{CS}_K} \alpha_i(t) |\psi_i\rangle, \quad (17)$$

where $\alpha_i(t) \in \mathbb{C}$. For the given selection of the Ansatz in equation 17, the second step of the QAS algorithm involves computing the overlap matrices. The matrix elements of \mathcal{D} and \mathcal{E} can be estimated efficiently on a quantum computer, using the techniques from Mitarai et al., without any complicated measurement such as the Hadamard test [26]. If the Hamiltonian is a linear combination of tensored Pauli operators, the elements can be directly inferred from the measurement in the corresponding computational basis. See Appendix E for details. Once the overlap matrices have been computed, the job of the quantum computer is over. The third (and final) step of the QAS algorithm involves solving the differential equation and parameter update using equations 15 and 16 on a classical computer. If the desired accuracy has not been attained, one can re-run the whole algorithm for a different choice of K .

Justification for the Ansatz— We now proceed to provide a small justification for the choice of the Ansatz in the QAS algorithm. Suppose the initial state (0-moment state) is $|\psi\rangle$. Starting with $|\psi\rangle$, if one applies $\exp(-iHt)$ for some $t \geq 0$, the evolved state is given by

$$|\gamma\rangle = e^{-iHt} |\psi\rangle. \quad (18)$$

Using $e^{-iHt} = \sum_{p=0}^{\infty} \frac{(-iHt)^p}{p!}$, we get

$$|\gamma\rangle = \sum_{p=0}^{\infty} \frac{(-iHt)^p}{p!} |\psi\rangle. \quad (19)$$

Let us define the operator

$$\mathcal{O}^K \equiv \sum_{p=0}^K \frac{(-iHt)^p}{p!}, \quad (20)$$

for $K \geq 0$. Notice that \mathcal{O}^K corresponds to the sum of first K terms of e^{-iHt} . Using \mathcal{O}^K , we proceed to define

$$|\gamma_K\rangle \equiv \frac{\sum_{p=0}^K \frac{(-iHt)^p}{p!} |\psi\rangle}{\langle\psi| \left(\sum_{p=0}^K \frac{(-iHt)^p}{p!} \right)^2 |\psi\rangle}. \quad (21)$$

For $K \rightarrow \infty$, $|\gamma_K\rangle \rightarrow |\gamma\rangle$. Using the expression for Hamiltonian as linear combination of unitary, it is easy to see that $|\gamma_K\rangle$ can be written as linear combination of cumulative K -moment states, i.e.,

$$|\gamma_K\rangle = \sum_{|u_i\rangle \in \mathbb{CS}_K} \alpha_i |u_i\rangle$$

where the combination coefficients $\alpha_i \in \mathbb{C}$. The aforementioned arguments justify the choice of Ansatz as linear combination of cumulative K -moment states. One may suspect that the accuracy of the algorithm improves with increasing K . However, depending on the algebra of the unitaries defining the Hamiltonian, this might not be true in general.

Examples— We now show examples of the QAS algorithm applied to various Hamiltonians and Ansatz states. First, in Fig.2, we investigate two elementary examples. In Fig.2a, we show the evolution with QAS of a single qubit for the Hamiltonian $H_B = \sigma^z$. In step 1 of the QAS algorithm, we choose the initial Ansatz state $|\psi\rangle = |\psi_0\rangle = |+\rangle$ (0-moment state) $\mathbb{S}_0 = \{|\psi_0\rangle\}$. Then, following Definition 1, we use the set of unitaries that make up the Hamiltonian $\{\sigma^z\}$ and generate the 1-moment states $\mathbb{S}_1 = \{|\psi_1\rangle\}$ with $|\psi_1\rangle = \sigma^z |\psi_0\rangle$. The union of \mathbb{S}_1 and \mathbb{S}_2 gives us the cumulative 1-moment states $\mathbb{CS}_1 = \{|\psi_0\rangle, |\psi_1\rangle\}$. Higher orders K of the moment expansion can be prepared by repeating this approach. In step 2, we calculate the overlap matrices $\mathcal{D}_{n,m} = \langle\psi_n| H_B |\psi_m\rangle$, $\mathcal{E}_{n,m} = \langle\psi_n| \psi_m\rangle$ (Eq.9, 11). Then, in step 3, we choose initial state of evolution $|\phi(t=0)\rangle = |\psi\rangle$ with $\alpha_0(0) = 1$ and $\alpha_1(0) = 0$, and then evolve $\alpha(t)$ to get the superposition state $|\phi(t)\rangle = \alpha_0(t) |\psi_0\rangle + \alpha_1(t) |\psi_1\rangle$. We show

the evolution of the expectation value of the Pauli operator $\langle \sigma^x(t) \rangle = \langle \phi(t) | \sigma^x | \phi(t) \rangle$. We find that the simulation with QAS and the exact evolution matches for the first moment expansion, i.e. $K = 1$.

Next, in Fig.2b, we prepare as Ansatz state a deep variational circuit, parameterized by angles θ and state $|\Psi(\theta)\rangle$. These circuits are highly expressive, however for random initialisation of θ , they form a Haar random state and suffer from the so-called barren plateaus [12]. Here, the variance of the gradients of the circuit in respect to the underlying cost function (say H) vanishes exponentially with the number of qubits N , i.e. $\text{var}(\partial_\theta \langle \Psi(\theta) | H | \Psi(\theta) \rangle) \propto \exp(-N)$. We now use the Ansatz studied in [12] for random variational states consisting of N qubits with $d \gg 1$ layers, composed of alternating single-qubit rotations around randomly chosen x -, y - or z -axis parameterized with angles θ and C-phase gates arranged in a hardware efficient manner. For gradient based methods, evolving this state is difficult as the gradients become exponentially small with increasing N . We now evolve this state with the Hamiltonian $H_{\text{bp}} = \sigma_1^z \sigma_2^z$ as chosen by Ref.[12]. We can already reproduce the time evolution of this state for the first moment expansion, i.e. $K = 1$.

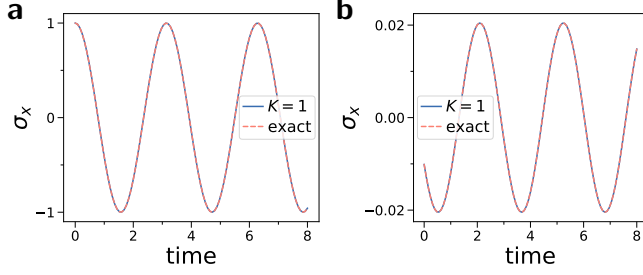


FIG. 2. Time evolution with QAS. **a)** Evolution of expectation value of $\langle \sigma^x(t) \rangle$ for single qubit with Hamiltonian $H_B = \sigma^z$. We show the simulation using first moment expansion and the exact result. **b)** Deep deep variational Ansatz for $N = 12$ qubits that exhibits barren plateaus for the gradients. It consists of $d = 200$ layers composed of alternating parameterized single-qubit rotations around randomly chosen x -, y - or z -axis and C-phase gates arranged in a hardware efficient manner [12]. We choose Hamiltonian $H_{\text{bp}} = \sigma_1^z \sigma_2^z$. We show evolution of expectation value of the first qubit $\langle \sigma_1^x(t) \rangle$ for both $K = 1$ moment expansion and the exact result.

Next, we discuss two further examples for the same variational Ansatz for different Hamiltonians in Fig.3. We evolve in Fig.3a this Ansatz with the Hamiltonian $H = \frac{1}{2}(\sigma^x[\otimes_{i=2}^{N-1} \sigma^z] \sigma^x + \sigma^y[\otimes_{i=2}^{N-1} \sigma^z] \sigma^y)$. After applying the Jordan-Wigner transformation [27], this Hamiltonian corresponds to a system of fermions tunneling from the first to the last site in a lattice system of length N with $H = c_1^\dagger c_N + c_N^\dagger c_1$, where c_i^\dagger (c_i) is the fermionic creation (annihilation) operator acting on site i . Evolving this Hamiltonian with naive implementations of Trotter can be difficult as it requires implementing a N -qubit rotation. We show fidelity of QAS with the exact evolu-

tion $F = |\langle \Psi_{\text{exact}}(t) | \phi(\alpha(t)) \rangle|^2$. We find optimal fidelity for moment $K = 2$. In Fig.3b we show the evolution of an exemplary many-body Hamiltonian, the Ising model. The Hamiltonian is given by

$$H_{\text{ising}} = \frac{J}{2} \sum_{i=1}^N \sigma_i^x \sigma_{i+1}^x + \frac{h}{2} \sum_{i=1}^N \sigma_i^z, \quad (22)$$

which describes an N spin system with nearest-neighbor coupled spins with amplitude J and an applied transverse magnetic field h . We find increasing fidelity with increasing K , matching for $K \geq 3$ the exact evolution.

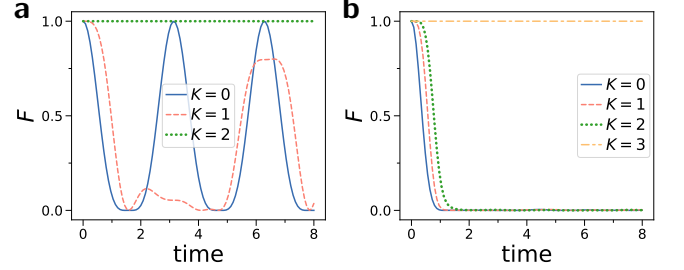


FIG. 3. Fidelity $F = |\langle \Psi_{\text{exact}}(t) | \phi(\alpha(t)) \rangle|^2$ against evolution time for deep random parameterized circuit using Ansatz of [12] for depth of circuit $d = 200$ and for varying moment expansion K . **a)** Hamiltonian $H = \frac{1}{2}(X[\otimes_{i=2}^{N-1} Z]X + Y[\otimes_{i=2}^{N-1} Z]Y)$, which can represent tunneling of fermionic particles between first and last site in a chain of $N = 10$ sites. **b)** Ising Hamiltonian for $N = 8$ sites with $J = 1, h = 1$.

Now, we discuss QAS for dynamical simulation of a chemistry problem. In Fig.4, we show the evolution of an excited state of a LiH molecule. We find that at $K = 1$ moment, the dynamics can be fully reproduced with QAS.

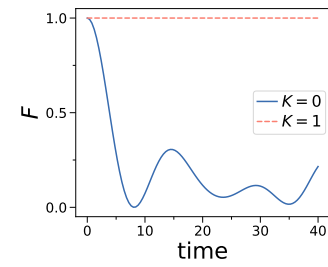


FIG. 4. LiH molecule evolution for a perturbed excited state (we choose equal superposition state of 10 lowest energy eigenstates). We show fidelity $F = |\langle \Psi_{\text{exact}}(t) | \phi(\alpha(t)) \rangle|^2$ against evolution time. The LiH molecule is mapped to 6 qubits using STO-3G basis using methods of [10], resulting in a Hamiltonian with 174 terms.

Finally, we discuss imaginary time evolution with QAS. We defer the details to Appendix C. In Fig.5, we show the energy $\langle H(t) \rangle$ of the imaginary time evolution of the Ising model for the deep variational Ansatz introduced above. With longer evolution time, the energy of

the quantum state decreases, until it reaches a minimal value. The found minimal energy decreases with increasing K , reaching the exact ground state for $K = 3$.

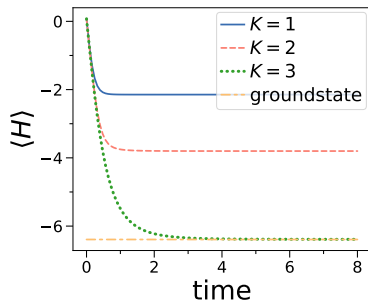


FIG. 5. Imaginary time evolution of energy $\langle H(t) \rangle$ for QAS. Simulation with $N = 10$ qubits ($J = 1$, $h = 1$) and randomized deep variational circuit as initial Ansatz state.

We show further examples for the simulated dynamics for a quenched many-body system in Appendix D.

Discussion and Conclusion— In this work, we provided a hybrid quantum-classical algorithm for simulating the dynamical evolution of a quantum system. Without loss of generality, we assume the Hamiltonian to be a linear combination of unitaries. Our algorithm proceeds in three steps and does not mandate any classical-quantum feedback loop. The first step of the algorithm involves the selection of the Ansatz. We consider our Ansatz to be a linear combination of quantum states, where the quantum states belong to the set of cumulative K -moment states, constructed using the unitaries defining the Hamiltonian. The combination coefficients are complex numbers in general. For the choice of the Ansatz in the first step, the second step involves the computation of two overlap matrices on the quantum computer. This step can be performed efficiently on existing quantum computers without the requirement of any complicated measurements. For a Hamiltonian consisting of a linear combination of Pauli strings, the measurement of the matrix elements only involves measurements of Pauli strings, which can be easily done on the existing hardware. See Appendix E for details. Once the overlap matrices have

been computed, the third (and final) step of the QAS algorithm involves solving the differential equation and updating the parameters corresponding to Eq. (15) and (16) on a classical computer. If the desired accuracy has not been attained, one can re-run the whole algorithm for a different choice of K .

Apart from Dirac and Frenkel variational principle, there are two other variational principles, which can be used for variational simulation of dynamics: the McLachlan variational principle [28] and the time-dependent variational method principle [29, 30]. For an Ansatz with complex adjustable parameters, all three variational principles lead to same dynamical evolution [23]. We also discussed the extension of our algorithm to imaginary time evolution (see appendix C for details). It is noteworthy to stress that the quantum states defining the Ansatz are fixed, and only the variational parameters are (classically) updated. The algorithm does not mandate the computation of gradients using the quantum computer and thus circumvents the barren plateau problem by construction. Our algorithm can be easily merged with VQS using the following Ansatz,

$$|\phi(\alpha(t), \theta)\rangle = \sum_{i=0}^{m-1} \alpha_i(t) |\psi_i(\theta_i)\rangle, \quad (23)$$

where $\alpha_i \in \mathbb{C}$ and $\theta_i \in \mathbb{R}$.

Since we unlock a fresh paradigm, there are many open questions for further investigation. In future, one could study the extension of our algorithm for simulating open system dynamics, in the presence of noise as well as for Gibbs state preparation. Extending our algorithm to simulate generalized time evolution is another exciting direction [31]. It would be interesting to provide complexity-theoretic guarantees as well as analyze the error in-depth. A proper study of the Ansatz construction is another exciting direction. We believe that an in-depth study of our algorithm will lead to the design of quantum-inspired classical algorithms for simulating the dynamics of quantum systems.

Acknowledgements— We are grateful to the National Research Foundation and the Ministry of Education, Singapore for financial support. We thank Jonathan for interesting discussions.

-
- [1] J. Preskill, Quantum **2**, 79 (2018).
 - [2] I. H. Deutsch, arXiv preprint arXiv:2010.10283 (2020).
 - [3] F. Arute, K. Arya, R. Babbush, D. Bacon, J. C. Bardin, R. Barends, R. Biswas, S. Boixo, F. G. Brandao, D. A. Buell, *et al.*, Nature **574**, 505 (2019).
 - [4] A. Peruzzo, J. McClean, P. Shadbolt, M.-H. Yung, X.-Q. Zhou, P. J. Love, A. Aspuru-Guzik, and J. L. O'Brien, Nature communications **5**, 4213 (2014).
 - [5] J. R. McClean, J. Romero, R. Babbush, and A. Aspuru-Guzik, New Journal of Physics **18**, 023023 (2016).
 - [6] A. Kandala, A. Mezzacapo, K. Temme, M. Takita, M. Brink, J. M. Chow, and J. M. Gambetta, Nature **549**, 242 (2017).
 - [7] E. Farhi, J. Goldstone, and S. Gutmann, arXiv:1411.4028 (2014).
 - [8] E. Farhi and A. W. Harrow, arXiv preprint arXiv:1602.07674 (2016).
 - [9] A. W. Harrow and A. Montanaro, Nature **549**, 203 (2017).
 - [10] S. McArdle, S. Endo, A. Aspuru-Guzik, S. C. Benjamin,

- and X. Yuan, *Reviews of Modern Physics* **92**, 015003 (2020).
- [11] S. Endo, Z. Cai, S. C. Benjamin, and X. Yuan, arXiv preprint arXiv:2011.01382 (2020).
 - [12] J. R. McClean, S. Boixo, V. N. Smelyanskiy, R. Babbush, and H. Neven, *Nature communications* **9**, 4812 (2018).
 - [13] H.-Y. Huang, K. Bharti, and P. Rebentrost, arXiv preprint arXiv:1909.07344 (2019).
 - [14] K. Sharma, M. Cerezo, L. Cincio, and P. J. Coles, arXiv preprint arXiv:2005.12458 (2020).
 - [15] M. Cerezo, A. Sone, T. Volkoff, L. Cincio, and P. J. Coles, arXiv preprint arXiv:2001.00550 (2020).
 - [16] S. Wang, E. Fontana, M. Cerezo, K. Sharma, A. Sone, L. Cincio, and P. J. Coles, arXiv preprint arXiv:2007.14384 (2020).
 - [17] C. O. Marrero, M. Kieferová, and N. Wiebe, arXiv preprint arXiv:2010.15968 (2020).
 - [18] K. Bharti, arXiv preprint arXiv:2009.11001 (2020).
 - [19] K. Bharti and T. Haug, arXiv preprint arXiv:2010.05638 (2020).
 - [20] D. Poulin, M. B. Hastings, D. Wecker, N. Wiebe, A. C. Doherty, and M. Troyer, arXiv:1406.4920 (2014).
 - [21] Y. Li and S. C. Benjamin, *Physical Review X* **7**, 021050 (2017).
 - [22] S. McArdle, T. Jones, S. Endo, Y. Li, S. C. Benjamin, and X. Yuan, *npj Quantum Information* **5**, 1 (2019).
 - [23] X. Yuan, S. Endo, Q. Zhao, Y. Li, and S. C. Benjamin, *Quantum* **3**, 191 (2019).
 - [24] P. A. Dirac, in *Mathematical Proceedings of the Cambridge Philosophical Society*, Vol. 26 (Cambridge University Press, 1930) pp. 376–385.
 - [25] I. Frenkel *et al.*, (1934).
 - [26] K. Mitarai and K. Fujii, *Physical Review Research* **1**, 013006 (2019).
 - [27] P. Jordan and E. P. Wigner, in *The Collected Works of Eugene Paul Wigner* (Springer, 1993) pp. 109–129.
 - [28] A. McLachlan, *Molecular Physics* **8**, 39 (1964).
 - [29] P. Kramer and M. Saraceno, in *Group Theoretical Methods in Physics* (Springer, 1980) pp. 112–121.
 - [30] J. Broeckhove, L. Lathouwers, E. Kesteloot, and P. Van Leuven, *Chemical physics letters* **149**, 547 (1988).
 - [31] S. Endo, J. Sun, Y. Li, S. C. Benjamin, and X. Yuan, *Phys. Rev. Lett.* **125**, 010501 (2020).

Appendix A: Error Analysis

The error accumulated during the time of evolution can be calculated by estimating the distance between the true evolution and the evolution of the Ansatz [23]. This is given by

$$\epsilon_t = \left\| \left(\frac{d}{dt} + \iota H \right) |\phi(\alpha(t))\rangle \right\|^2, \quad (\text{A1})$$

where $\|\xi\|^2 = \langle \xi | \xi \rangle$. Using equation A1, the error term ϵ_t is given by

$$\begin{aligned} \epsilon_t = & \sum_{i,j} \frac{\partial \langle \phi(\alpha(t)) |}{\partial \alpha_i} \frac{\partial |\phi(\alpha(t))\rangle}{\partial \alpha_j} \dot{\alpha}_i^* \dot{\alpha}_j + \\ & \iota \sum_i \frac{\partial \langle \phi(\alpha(t)) |}{\partial \alpha_i} H |\phi(\alpha(t))\rangle \dot{\alpha}_i^* \\ & - \iota \sum_i \langle \phi(\alpha(t)) | H \frac{\partial |\phi(\alpha(t))\rangle}{\partial \alpha_i} \dot{\alpha}_i + \\ & \langle \phi(\alpha(t)) | H^2 | \phi(\alpha(t)) \rangle. \quad (\text{A2}) \end{aligned}$$

Appendix B: Realification

Recall that the Ansatz evolution equation is given by

$$\mathcal{E} \frac{\partial \alpha(t)}{\partial t} = -\iota \mathcal{D} \alpha(t), \quad (\text{B1})$$

where $\alpha_i(t) \in \mathbb{C}$. Moreover, the overlap matrices \mathcal{E} and \mathcal{D} can be in general complex. We can use realification to solve the above differential equation for $\alpha(t)$. The idea of realification is to create a mapping from \mathbb{C}^n to \mathbb{R}^{2n} . The crux of the idea is the following real matrix representation for 1 and i ,

$$1 \leftrightarrow \begin{bmatrix} 1 & 0 \\ 0 & 1 \end{bmatrix} \equiv \mathbb{I} \quad (\text{B2})$$

and

$$i \leftrightarrow \begin{bmatrix} 0 & -1 \\ 1 & 0 \end{bmatrix} \equiv I. \quad (\text{B3})$$

It can be seen that $I^2 = -\mathbb{I}$, which mimics $i^2 = -1$. Let $\mathcal{E}_{\mathcal{R}}$, $\mathcal{D}_{\mathcal{R}}$ and $\mathcal{E}_{\mathcal{I}}$, $\mathcal{D}_{\mathcal{I}}$ be the real and imaginary parts of the overlap matrices \mathcal{E} and \mathcal{D} . Let $\alpha_{\mathcal{R}}(t)$ and $\alpha_{\mathcal{I}}(t)$ be the real and imaginary parts of $\alpha(t)$. Using the mappings in B2 and B3, one can obtain the following representation for

$$\mathcal{E} = \begin{bmatrix} \mathcal{E}_{\mathcal{R}} & -\mathcal{E}_{\mathcal{I}} \\ \mathcal{E}_{\mathcal{I}} & \mathcal{E}_{\mathcal{R}} \end{bmatrix}, \quad (\text{B4})$$

$$\mathcal{D} = \begin{bmatrix} \mathcal{D}_{\mathcal{R}} & -\mathcal{D}_{\mathcal{I}} \\ \mathcal{D}_{\mathcal{I}} & \mathcal{D}_{\mathcal{R}} \end{bmatrix}, \quad (\text{B5})$$

and

$$\alpha(t) = \begin{bmatrix} \dot{\alpha}_R(t) & -\dot{\alpha}_I(t) \\ \dot{\alpha}_I(t) & \dot{\alpha}_R(t) \end{bmatrix}. \quad (\text{B6})$$

Using the above representation, one trivially gets the following realified evolution equation.

$$\begin{bmatrix} \mathcal{E}_R & -\mathcal{E}_I \\ \mathcal{E}_I & \mathcal{E}_R \end{bmatrix} \begin{bmatrix} \dot{\alpha}_R(t) \\ \dot{\alpha}_I(t) \end{bmatrix} = \begin{bmatrix} \mathcal{D}_R & -\mathcal{D}_I \\ \mathcal{D}_I & \mathcal{D}_R \end{bmatrix} \begin{bmatrix} \alpha_R(t) \\ \alpha_I(t) \end{bmatrix}. \quad (\text{B7})$$

Appendix C: Imaginary Time Evolution

Substituting t with $-\iota\tau$ in Eq.(1) we get

$$\frac{d|\psi(\tau)\rangle}{d\tau} = -(H - \langle H \rangle) |\psi(\tau)\rangle, \quad (\text{C1})$$

where $\langle H \rangle = \langle \psi(\tau) | H | \psi(\tau) \rangle$. The presence of $\langle H \rangle$ preserves the norm of $|\psi(\tau)\rangle$. Let us consider the Ansatz state as linear combination of m quantum states $\{|\psi_i\rangle\}_i$

$$|\phi(\alpha(\tau))\rangle = \sum_{i=0}^{m-1} \alpha_i(\tau) |\psi_i\rangle, \quad (\text{C2})$$

for $\alpha_i(\tau) \in \mathbb{C}$. Using Dirac and Frenkel variational principle, we get

$$\langle \delta\phi(\alpha(\tau)) | \left(\frac{d}{d\tau} + H - \langle H \rangle \right) |\phi(\alpha(\tau))\rangle = 0, \quad (\text{C3})$$

where

$$\langle \delta\phi(\alpha(\tau)) | = \sum_i \frac{\partial \langle \phi(\alpha(\tau)) |}{\partial \alpha_i} \delta \alpha_i. \quad (\text{C4})$$

The evolution of parameters is given by

$$\sum_j \mathcal{E}_{i,j} \dot{\alpha}_j = -\mathcal{G}_i, \quad (\text{C5})$$

where \mathcal{E} and \mathcal{G} are

$$\mathcal{E}_{i,j} = \frac{\partial \langle \phi(\alpha(\tau)) |}{\partial \alpha_i} \frac{\partial \langle \phi(\alpha(\tau)) |}{\partial \alpha_j}, \quad (\text{C6})$$

$$\mathcal{G}_i = \sum_j \alpha_j(\tau) \frac{\partial \langle \phi(\alpha(\tau)) |}{\partial \alpha_i} (H - \langle H \rangle) |\psi_j\rangle. \quad (\text{C7})$$

Further simplification leads to

$$\begin{aligned} \mathcal{G}_i &= \left(\sum_j \alpha_j(\tau) \langle \psi_i | H | \psi_j \rangle \right) - \langle H \rangle \left(\sum_j \alpha_j(\tau) \langle \psi_i | \psi_j \rangle \right) \\ \Rightarrow \mathcal{G}_i &= \sum_j \mathcal{D}_{i,j} \alpha_j(\tau) - \langle H \rangle \sum_j \mathcal{E}_{i,j} \alpha_j(\tau). \end{aligned} \quad (\text{C8})$$

Appendix D: Quantum Quench

We now give further numerical examples for QAS. We demonstrate quench dynamics for many-body systems. Here, the system is prepared in the ground state of a Hamiltonian. Then, to generate the dynamics, the parameters of the Hamiltonian are instantaneously changed to another value. We show two examples for such dynamics in Fig.6. We study the Ising Hamiltonian given by

$$H_{\text{ising}} = \frac{J}{2} \sum_{i=1}^N \sigma_i^x \sigma_{i+1}^x - \frac{h}{2} \sum_{i=1}^N \sigma_i^z, \quad (\text{D1})$$

and the Heisenberg model

$$H_{\text{Xxz}} = \frac{1}{2} \sum_{i=1}^N (\sigma_i^x \sigma_{i+1}^x + \sigma_i^y \sigma_{i+1}^y + \Delta \sigma_i^z \sigma_{i+1}^z) \quad (\text{D2})$$

which describe N spin systems with nearest-neighbor coupled spins with parameters J and h . We find that for the Ising Hamiltonian (Fig.6a), the evolution becomes more accurate with increasing K , reaching optimal fidelity for $K = 4$. In Fig.6b, we study the Heisenberg model. We find that we converge to optimal fidelity for $K \geq 3$.

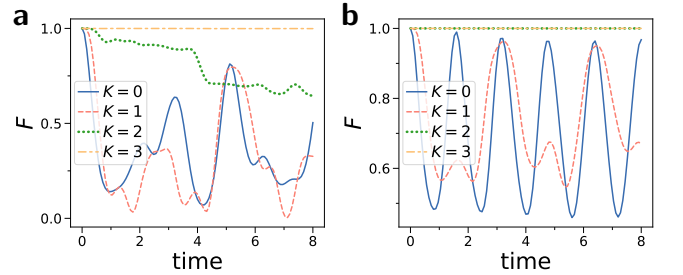


FIG. 6. Many-body quench against time with fidelity $F = |\langle \Psi_{\text{exact}}(t) | \phi(\alpha(t)) \rangle|^2$ in respect to exact dynamics for varying moment expansion K . **a)** Ising Hamiltonian. **b)** Heisenberg model. In both cases, we prepare the initial ground state of Hamiltonian with $J = 1$, $h = 0.5$, and then quench the Hamiltonian parameter instantaneously to $h = 2$. Number of qubits is $N = 8$.

Appendix E: Measurements

We reiterate here the content from reference [19]. For the purposes of this section, a unitary U will be referred k -local if it acts non-trivially on at most k qubits. We assume $k = \mathcal{O}(\text{poly}(\log(N)))$. The moment- K Ansatz, for some positive integer K , in QAS algorithm requires computation of matrix elements of the form $\langle \psi | U | \psi \rangle$, where U is a k -local unitary matrix (since U is product of at most $2K + 1$ k -local unitary matrices). By invoking the following result from Mitarai *et. al.* [26], we guarantee an efficient computation of the overlap matrices on

a quantum computer without the use of the Hadamard test.

Fact 2. [26] Let k be an integer such that $k = \mathcal{O}(\text{poly}(\log(N)))$, where N is the number of qubits and $|\psi\rangle$ be an N -qubit quantum state. For any k -local quantum gate U , it is possible to estimate $\langle\psi|U|\psi\rangle$ up to precision ϵ in time $\mathcal{O}(k^{2^{2k}}/\epsilon^2)$ without the use of the Hadamard test, with classical preprocessing of time $\mathcal{O}(\text{poly}(\log N))$.

We proceed to discuss the methodology suggested in [26] to calculate the required matrix elements. For detailed analysis, refer to [26]. Since U is a k -local unitary, it can be decomposed as $U = \bigotimes_{q=1}^Q U_q$ such that U_q acts on k_q qubits. Clearly, U_q is a $2^{k_q} \times 2^{k_q}$ matrix. Suppose the eigenvalues of U_q are $\{\exp(i\phi_{q,m})\}_{m=0}^{2^{k_q}-1}$. Using the integers $m_q = 0, \dots, 2^{k_q}-1$, let us denote the computational basis of each subsystem by $|m_q\rangle$. We diagonalize each U_q and obtain some unitary matrix V_q such that $U_q = V_q^\dagger T_q V_q$, where $T_q = \sum_{m=0}^{2^{k_q}-1} \exp(i\phi_{q,m})$. Since $k = \mathcal{O}(\text{poly}(\log(N)))$, the aforementioned diagonalization can be performed in polynomial time. A simple calculation gives,

$$\langle\psi|U|\psi\rangle = \sum_{m_1=0}^{2^{k_1}-1} \cdots \sum_{m_Q=0}^{2^{k_Q}-1} \left(\prod_{q=1}^Q \exp(i\phi_{q,m_q}) \right) \times \left| \left(\bigotimes_{q=1}^Q \langle m_q | \right) \left(\bigotimes_{q=1}^Q V_q \right) |\psi\rangle \right|^2. \quad (\text{E1})$$

Thus, one can evaluate $\langle\psi|U|\psi\rangle$ by calculating the probability of getting $\bigotimes_{q=1}^Q |m_q\rangle$ from the measurement of $\left(\bigotimes_{q=1}^Q V_q \right) |\psi\rangle$ in the computational basis.

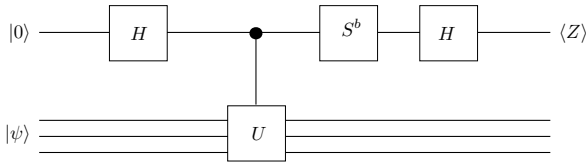


FIG. 7. The above figure shows a simple Hadamard test circuit for measuring the real and imaginary part of $\langle\psi|U|\psi\rangle$ for any arbitrary n qubit unitary U . The Hadamard gate has been represented by H and S represents $e^{-i\pi Z/4}$. When $b = 0$, we get $\langle Z \rangle = \text{Re} \langle\psi|U|\psi\rangle$. For $b = 1$, we get $\langle Z \rangle = \text{Im} \langle\psi|U|\psi\rangle$. Since implementing controlled-unitaries is challenging in the NISQ era, the use of Hadamard test as a subroutine is highly discouraged while designing NISQ-friendly quantum algorithms. Using results from [26], we guarantee an efficient computation of the overlap matrices required in the QAS algorithm on a quantum computer without the use of the Hadamard test.

If the unitaries defining the Hamiltonian are Pauli strings over N qubits, one can use the following Lemma

[13] to provide an estimate of the number of measurements needed to achieve a given desired accuracy.

Lemma 3. [13] Let $\epsilon > 0$ and P_q be a Pauli string over N qubits. Let multiple copies of an arbitrary N -qubit quantum state $|\psi\rangle$ be given. The expectation value $\langle\psi|P_q|\psi\rangle$ can be determined to additive accuracy ϵ with failure probability at most δ using $\mathcal{O}(\frac{1}{\epsilon^2} \log(\frac{1}{\delta}))$ copies of $|\psi\rangle$.

We now discuss how to measure the matrix elements of \mathcal{D} and \mathcal{E} for the special case where the components U_i of the Hamiltonian $H = \sum_i \beta_i U_i$ are Pauli strings $P_q = \bigotimes_{j=1}^N \gamma_j$, with $\gamma \in \{\mathbb{1}, \sigma^x, \sigma^y, \sigma^z\}$. For a K -moment state expansion of Ansatz $|\Psi\rangle$, the elements to calculate are

$$\mathcal{D}_{n,m} = \sum_i \beta_i \langle\Psi|U_{n_1}^\dagger \cdots U_{n_K}^\dagger U_i U_{m_K} \cdots U_{m_1} |\Psi\rangle$$

$$\mathcal{E}_{n,m} = \langle\Psi|U_{n_1}^\dagger \cdots U_{n_K}^\dagger U_{m_K} \cdots U_{m_1} |\Psi\rangle. \quad (\text{E2})$$

Now, each overlap element is a product of a set of some Pauli strings P_q to be measured on state $|\Psi\rangle$, with $\langle\Psi|\prod_q P_q|\Psi\rangle$. The product rule of Pauli operators states that $\sigma^i \sigma^j = \delta_{ij} \mathbb{1} + i\epsilon_{ijk} \sigma^k$, where $\sigma^1 = \sigma^x$, $\sigma^2 = \sigma^y$, $\sigma^3 = \sigma^z$, δ_{ij} is the Kronecker delta and ϵ_{ijk} the Levi-Civita symbol. Thus, a product of two Pauli strings $P_q P_p = a P_s$ is again a Pauli string P_s , with a prefactor $a \in \{+1, -1, +i, -i\}$. To calculate the matrix elements on the quantum computer, first one has to evaluate which Pauli string corresponds to the product of unitaries in Eq. E2 and the corresponding prefactor. Then, the expectation value of the resulting Pauli string is measured for the Ansatz state $\langle\Psi|P_q|\Psi\rangle$. This observable is a hermitian operator, and can be easily measured by rotating each qubit into the computational basis corresponding to the Pauli operator. Finally, the expectation value of the measurement is multiplied with the prefactor a .